Journal of Materials Chemistry B

Accepted Manuscript

This is an *Accepted Manuscript*, which has been through the Royal Society of Chemistry peer review process and has been accepted for publication.

Accepted Manuscripts are published online shortly after acceptance, before technical editing, formatting and proof reading. Using this free service, authors can make their results available to the community, in citable form, before we publish the edited article. We will replace this *Accepted Manuscript* with the edited and formatted *Advance Article* as soon as it is available.

You can find more information about *Accepted Manuscripts* in the Information for Authors.

Please note that technical editing may introduce minor changes to the text and/or graphics, which may alter content. The journal's standard Terms & Conditions and the Ethical guidelines still apply. In no event shall the Royal Society of Chemistry be held responsible for any errors or omissions in this *Accepted Manuscript* or any consequences arising from the use of any information it contains.

ROYAL SOCIETY OF CHEMISTRY

www.rsc.org/materialsB

Photoactivation of Core-Shell Titania Coated Upconversion Nanoparticles and its Effect on Cell Death

Niagara Muhammad Idris[1], *Sasidharan Swarnalatha Lucky*[1], *Zhengquan Li*[2], *Kai Huang*[1] *and Yong Zhang*[1,]*

[1]Department of Biomedical Engineering, National University of Singapore, Singapore 117575

[2]Department of Materials Physics, Zhejiang Normal University, Zhejiang 321004, P. R. China

Keywords: Titanium dioxide; upconversion; near-infrared; reactive oxygen species; photodynamic therapy.

Abstract

Titania (TiO_2) has been explored as a potential drug in eradicating cancer by virtue of its photocatalytic property to generate reactive oxygen species (ROS) under UV irradiation. Its clinical application, however, has been hampered by the tissue penetration depth limit of the UV light needed for its activation. The use of 'invisible' near-infrared (NIR) light affords greater tissue penetration depth because most tissues are 'transparent' to NIR light. Here, we uniformly coated TiO_2 to a nanometer-sized light transducer that can upconvert highly penetrating NIR light to the activation absorption spectrum of TiO_2 at UV range. Under NIR excitation, photoinduced TiO_2 by the upconverted UV light results in the generation of more than one type of ROS that was stably produced under an appropriate storage condition. The amount of ROS produced was also effective in killing cancer cells *in vitro*, thus suggesting its potential in overcoming the current penetration depth limit.

Journal of Materials Chemistry B Accepted Manuscript

1. Introduction

Nanoparticles are emerging as promising agents for cancer therapy, backed by wide-ranging mechanisms of cell destruction that include acting as carriers for chemotherapeutics,[1] as thermal coupling agents for hyperthermia and photothermal therapy[2] and also as photosensitizing agents for photodynamic therapy (PDT).[3] In PDT, the nanoparticles may serve as a carrier of photosensitizer drugs or act as the photosensitizer drug themselves. The photosensitizer becomes activated when irradiated with a suitable light, to generate toxic reactive oxygen species (ROS) that can be exploited to kill cancer cells for tumor eradication. Discovery of the Honda-Fujishima Effect[4] that first revealed the photocatalytic properties of titania (TiO_2), has sparked off an interest in the use of this semiconductor as a detoxifying and disinfecting agent for the decomposition of a wide variety of contaminants.[5-9] The mechanism of decomposition relies on absorbing UV light that has an energy greater than the TiO_2 band gap. Under such UV illumination, TiO_2 is excited such that electron from its valence band gets promoted to the conduction band to generate a highly reactive electron-hole (e^--h^+) pair.[4] The electron and hole can reduce or oxidize chemical species on the surface of the TiO_2, hence effectively breaking them down into innocuous materials. In recent years, there has been growing interest in using TiO_2 nanoparticles as a drug in PDT to kill cancer cells.[10-16] However, TiO_2's requirement for activation by UV light has been a major impediment to its practical clinical usage. Besides causing damage to cells and tissues, UV light is strongly absorbed and scattered by tissues, thereby limiting its penetration depth to only fractions of a millilitre.[17, 18] Clinical application of TiO_2 would thus be restricted only to superficial malignancies, or those at cavitary sites whose accessibility could only be reached by optical fibers delivering the UV light. Apparently, deep penetration into tissues can be attained by light in the NIR region (700 – 1100 nm), due to its less scattering and absorption by tissues at this longer wavelength range.[19] In order to match this deeply penetrating NIR light to the activation absorption spectrum of TiO_2 at UV range, a light transducer that can convert NIR

Journal of Materials Chemistry B Accepted Manuscript

to UV light is thus required. Nano-materials made of rare earth metals have this unique ability to absorb NIR light and emit higher energy light in the UV/visible spectrum based on the process termed 'upconversion'.[20] Besides utilizing safe and deeply penetrating NIR light, these upconversion nanoparticles (UCN) are endowed with the advantage of highly unusual optical properties such as absolute photostability, near-zero autofluorescence background and tunable emission colors to suit different activation wavelengths of diverse photoactivable compounds.[21-27] These make them a conveniently versatile yet powerful tool for diverse photoactivation and imaging applications.[28-30] Nanocomposites of UCN and TiO_2 have been demonstrated as feasible producers of ROS under NIR excitation.[31-34] However, most of them show non-uniformity in size and dispersion as well as irregularity in shape.[32, 33] In the present study, a continuous layer of TiO_2 is individually coated on each UCN core to give rise to a defined core-shell structure with uniform size, shape and dispersion. We examined the stability of the TiO_2-UCN to produce ROS under different storage conditions, the type of ROS produced, as well as their potential as an agent of PDT *in vitro*.

2. Results and Discussion

As shown in **Figure 1a**, $NaYF_4$ nanocrystal co-doped with lanthanide ions Yb and Tm forms the core of the nanoconstruct while a layer of TiO_2 is coated over it to yield the resultant core-shell TiO_2-UCN. Powder X-ray diffraction (XRD) pattern and energy dispersive X-ray (EDX) spectroscopy analysis collected from the core-shell nanoconstruct ascertained this. As seen in **Figure 1b**, the peaks from the XRD pattern of the core particles can be indexed to $NaYF_4$ nanocrystal[35] while that of core-shell particles can be indexed to both $NaYF_4$ nanocrystal and anatase phase TiO_2 (JCPDS standard card no. 21-1272), indicating deposition of TiO_2 layer on the core-shell particles. The composition of these core-shell particles was further confirmed by their EDX spectrum as displayed in **Figure 1c**. The UCN core acts as a light transducer while the TiO_2 shell serves as a photocatalyst. Under 980 nm NIR excitation, the UCN

Journal of Materials Chemistry B Accepted Manuscript

upconverts the 980 nm light to UV and visible light of different wavelengths (**Figure 1d**). Spectral overlap between the emitted UV and absorption wavelength of the coated TiO_2[36] activates the TiO_2 layer to generate several cytotoxic ROS (**Figure 1e**) including hydroxyl radical, superoxide anion and hydrogen peroxide that can be used to kill cancer cells for PDT (**Figure 1f**). Investigation on the stability of these TiO_2-UCN to fluoresce under 980 nm NIR excitation when suspended in different physiological solutions such as water, phosphate buffered saline (PBS) and Dulbecco's Modified Eagle Medium (DMEM) with or without serum supplementation, revealed no obvious difference in the intensity of their emission fluorescence (**Figure 2a**). Interestingly, this photostability feature of the particles were also observed when they were soaked in acidic water with a pH of 4 for up to 3.5 h, albeit showing a small drop in fluorescence intensity when compared to soaking in water (with a pH of ~6.5) for the same time duration (**Figure 2b**). This may find useful implications when the particles are endocytosed into an acidic compartment of the cell such as endosomes and lysosomes in subsequent downstream biological applications.

As shown previously in Figure 1e, TiO_2-UCN successfully produced ROS upon NIR irradiation. Here, we used the dye aminophenyl fluorescein (APF) as a ROS indicator that remained nonfluorescent until oxidized with a ROS molecule to emit a green fluorescence. We measured this fluorescence of the dye in water in the presence of different amount of TiO_2-UCN irradiated at 980 nm and saw an obvious increase in the APF dye fluorescence with a corresponding increase in the amount of irradiated TiO_2-UCN (Figure 1e). To determine the type of ROS that is produced from these NIR-irradiated TiO_2-UCN suspended in water, we performed a series of scavenger experiments. Sodium pyruvate, dimethyl sulfoxide (DMSO), Tiron and sodium azide – the respective scavengers for hydrogen peroxide, hydroxyl radical, superoxide anion and singlet oxygen – were individually added into the suspension of TiO_2-UCN irradiated with the 980 nm laser. Fluorescence quenching of the APF dye upon addition of the respective scavenger would denote presence of a particular

Journal of Materials Chemistry B Accepted Manuscript

type of ROS. As shown in **Figure 3a-c**, significant fluorescence quenching was seen in samples containing the scavengers sodium pyruvate, DMSO and Tiron (P = 0.02328, 0.00766 and 0.00317, respectively, compared to irradiated TiO_2-UCN without scavenger addition), while that having the scavenger sodium azide showed no such quenching of the APF dye (**Figure 3d**). This indicates that photoinduced TiO_2-UCN produced more than one type of ROS and that includes hydrogen peroxide, hydroxyl radical and superoxide anion. Although the result suggests that singlet oxygen was not generated, fluorescence enhancement of the APF dye observed upon addition of the scavenger sodium azide is rather surprising. To circumvent possible confounding results, the study was verified by another test that used a fluorogenic marker specific only towards singlet oxygen – the singlet oxygen sensor green dye. The test detected no fluorescence increase of the singlet oxygen sensor green dye from NIR-irradiated TiO_2-UCN suspension (**Figure 3e**), corroborating previous result from the scavenger experiment in that no singlet oxygen was produced from the NIR-irradiated TiO_2-UCN. Indeed, this is in contrast to conventional PDT that kills cancer cells by singlet oxygen produced from photosensitizer irradiated with direct visible light. This may have implication on the mechanism in which TiO_2-UCN-mediated PDT kills cells and that it may be different from conventional PDT. When exposed to UV light that has an energy greater than its bandgap, TiO_2 is excited such that electron from its valence band gets promoted to the conduction band to generate a highly reactive electron-hole (e^--h^+) pair.[4] The electron and hole can reduce or oxidize O_2 and H_2O molecules on the surface of the TiO_2 to generate ROS. Typically, reduction of O_2 would generate superoxide anion radical and hydrogen peroxide while oxidation of H_2O would produce hydroxyl radicals.[37-39] Compared to these ROS, the amount of singlet oxygen that can be produced by direct energy transfer from photoinduced TiO_2 to surrounding O_2 is generally not substantial. This is due to a large mismatch between the bandgap energy of TiO_2 and the excitation energy of oxygen, thereby resulting in the semiconductor's low efficiency in photogenerating singlet oxygen.[40] Undeniably, however,

Journal of Materials Chemistry B Accepted Manuscript

there have been reports that detected enhanced singlet oxygen generation with relatively high quantum yield from certain forms of TiO_2.[41-44] Apparently, the efficiency of TiO_2 in photogenerating singlet oxygen largely depends on its particle size and surrounding pH, with a higher amount of singlet oxygen being generated from TiO_2 particles with smaller size.[41, 45] The proposed mechanism behind the generation of singlet oxygen is a two-step process whereby O_2 would first be reduced to superoxide anion radical as in a typical TiO_2 photocatalytic reaction, followed by oxidation of the superoxide anion radical to singlet oxygen.[45] It can be speculated here that the nature and structure of the TiO_2 shell formed over the UCN in this study do not conform to the specific form of TiO_2 that has the ability in producing detectable level of singlet oxygen. Conventional dye photosensitizers, on the other hand, follow a different mechanistic route in generating ROS. Upon excitation by light of an appropriate wavelength that matches its maximum absorption wavelength, electrons of a dye photosensitizer get boosted to a higher energy level and convert it to a short-lived excited singlet state. In this state, it has the ability to undergo intersystem crossing whereby the spin of its excited electron gets inverted to form a relatively long-lived excited triplet-state.[46, 47] As the surrounding O_2 also exists as a triplet in its ground state, dye photosensitizer in the triplet state can directly transfer its energy to surrounding O_2 to form an excited state singlet oxygen.

We also examined whether storage conditions affect TiO_2-UCN activity for ROS production. Here, TiO_2-UCN activity for ROS production under 980 nm irradiation was monitored as it aged over 20 days as dry powder at different storage conditions of either 4 °C in the dark, room temperature (RT) in the dark or RT but exposed to light (**Figure 4a**). Aging of the TiO_2-UCN powder at 4 °C in the dark did not correlate to a marked decrease in its activity for ROS production. In stark contrast, storing it at RT either in the dark or with light exposure for the same time duration drastically lowered its activity for ROS production. Further attempt to investigate on whether lower temperature would influence the TiO_2-UCN activity for ROS production was also made by storing the nanoparticles as dry powder at -20

Journal of Materials Chemistry B Accepted Manuscript

°C for 4 days. When compared to those stored at 4 °C for the same time duration, no appreciable difference was observed in the TiO_2-UCN activity for ROS production (P = 0.4211 between storage at 4 °C and -20 °C) (**Figure S1**). It seems then that storage of the TiO_2-UCN powder in the fridge is sufficient in preserving its shelf life and that lower temperature such as that in the freezer is not necessarily better in this sense. With the optimum condition to preserve TiO_2-UCN activity for ROS production now being identified, its shelf life at this storage condition was next monitored. Although there was a fair bit of decline in TiO_2-UCN activity for ROS production in the first 10 days of storage at 4 °C, its level of activity became stabilized thereafter for up to 57 days of storage (P = 0.10247 between 0 day and 57 days of storage) (**Figure 4b**).

As these nanoparticles would subsequently be subjected to surface modification with molecules such as polyethylene glycol and cancer-specific targeting agent in later part of the study (that will help to improve its biocompatibility and targeting efficacy, respectively), their stability for ROS production when soaked in different solvents was assessed. This is based on the rationale that such surface modification step oftentimes require the nanoparticles to be in contact with a certain solvent for long hours in order for sufficient grafting/conjugation to take place. To investigate this, the nanoparticles were soaked overnight in either ethanol (EtOH), tetrahydrofuran (THF), toluene, chloroform or anhydrous DMSO. Their stability for ROS production before and after soaking in the different solvents was then compared. While soaking the nanoparticles in toluene, chloroform or anhydrous DMSO brings a sharp drop in their activity for ROS production (P = 0.01015, 0.00711 and 0.00746, respectively, compared to before soaking), soaking in EtOH or THF have no such effect on the nanoparticles (**Figure 4c**). In fact, the amount of ROS produced from nanoparticles soaked in either EtOH or THF seemed barely unchanged when compared to the amount of ROS produced before they were soaked in these solvents (P = 0.97243 and 0.85389, respectively, compared to before soaking).

Journal of Materials Chemistry B Accepted Manuscript

We can thus deduce that EtOH or THF is most apt as a solvent for subsequent surface modification step. Indeed, an extended study to examine the long-term effect of storing TiO_2-UCN in EtOH at 4 °C revealed a stable production of ROS (**Figure 4d**) and relatively uniform size dispersion (**Figure S2**) of the particles for over 4 weeks. The solvents used to soak the TiO_2-UCN in this study can be generally classified into polar and non-polar solvents, with DMSO, EtOH and THF belonging to the polar category while toluene and chloroform belonging to the latter category. The polarity of these solvents may have an effect on the photocatalytic property of TiO_2-UCN. Indeed, Mao *et al.* have studied this on the catalytic performance of a TiO_2-based catalyst and found that solvents with strong polarity deactivated the catalyst at a low rate as compared to those with weaker polarity.[48] Hence, this may explain for the sharp drop in ROS production from those TiO_2-UCN particles soaked in non-polar solvents like toluene and chloroform, but not in polar solvents like EtOH and THF. However, such an effect was not observed in DMSO. This might be due to the fact that although DMSO is a polar solvent, it is also a known scavenger for hydroxyl radical, one of the ROS that is being produced from our photoinduced TiO_2-coated nanoplatform. Since it is not easy to remove all traces of the solvent by evaporation prior to the ROS test, it is highly possible that remnants of DMSO adsorbed at the surface of the TiO_2-UCN would scavenge any hydroxyl radical that was formed, thus accounting for the sharp drop in ROS production from those particles soaked in DMSO.

As these nanoparticles are intended for subsequent use as a PDT agent in living cells and organisms that are mainly made up of aqueous solutions, their stability for ROS production when soaked in water for long duration was assessed. Here, the TiO_2-UCN powder was soaked in water at RT for 24 h during which their activity for ROS production was assessed. As evident in **Figure 5a**, TiO_2-UCN showed a gradual decline in their activity for ROS production when soaked in water but this reached statistical significance only at 24 h of soaking (P = 0.04225 at 24 h compared to 0 h of soaking in water). An effort to delay this

Journal of Materials Chemistry B Accepted Manuscript

gradual loss in activity for ROS production was attempted using the different storage condition approach. TiO_2-UCN powder that has aged for 20 days at different storage conditions of either 4 °C in the dark, RT in the dark or RT but exposed to light (from previous study indicated as Figure 4a and reproduced in this section as **Figure 5b**) was soaked in water and the suspension continued to be kept at their respective storage condition for 24 h. After which, their activity for ROS production was assessed (**Figure 5c**). It is apparent from **Figure 5d** that loss in activity for ROS production was best retarded when the nanoparticles in water was stored at 4 °C in the dark whereby ROS production dropped to only 77.3 % as compared to those stored at RT in the dark or RT but exposed to light wherein the drop in ROS production reached a considerable level of 46.8 % and 48.1 % respectively. In preserving its activity for ROS production, it is thus best if TiO_2-UCN suspension in aqueous solution be kept on ice while waiting for their administration into cells/animals.

The nanoparticles' ability as an agent of PDT was next examined *in vitro*. We observed clear uptake of TiO_2-UCN into oral squamous carcinoma cells (OSCC) after 6 h of incubation with the cancer cells (**Figure 6a**), which is important for subsequent PDT treatment. During the 6 h of incubation, OSCC exposed to TiO_2-UCN at a concentration of up to 270 μg mL^{-1} achieved a reasonable cell viability of at least 78 % of control untreated cells (**Figure 6b**). Although there is significant difference between control cells and those exposed to TiO_2-UCN at concentration between 27 to 270 μg mL^{-1} ($P < 0.05$), the percentage of cells that remained viable at these concentrations is above the limit at half maximal inhibitory concentration (IC_{50}). A similar result was obtained when the nanoparticles were incubated with a normal cell line, the normal human lung fibroblasts (NHF), with cell viability reaching at least 83 % of control untreated cells (Figure 6b). Under 980 nm irradiation though, a significant drop in cell viability to 42 to 47 % of control untreated cells was observed in both the cancer and normal cells incubated with TiO_2-UCN at concentration between 13.5 to 270 μg mL^{-1} ($P < 0.05$ between treatment with NIR laser and TiO_2-UCN versus treatment with

Journal of Materials Chemistry B Accepted Manuscript

TiO_2-UCN alone (i.e. dark-toxicity values) at their respective concentration) (**Figure 6c**), thus indicating effectiveness of the nanoparticles as an agent of PDT in inducing cell death.

3. Experimental

Synthesis of TiO_2-UCN: TiO_2-UCN was synthesized by a multistep process: 1) synthesis of $NaYF_4$:Yb,Tm core nanocrystals; 2) coating of a layer of amorphous silica onto the core nanocrystals; 3) final coating of a continuous layer of TiO_2. Synthesis of the core nanocrystal and its subsequent coating with a silica layer is similar as that reported previously[49 35]: YCl3 (0.8 mmol), YbCl3 (0.2 mmol) and TmCl3 (0.005 mmol) were mixed with 6 mL oleic acid and 15 mL octadecene in a 50 mL flask. The solution was heated to 160 °C to form a homogeneous solution, and then cooled down to RT. 10 mL of methanol solution containing NaOH (2.5 mmol) and NH_4F (4 mmol) was slowly added into the flask and stirred for 30 min. Subsequently, the solution was slowly heated to remove methanol, degassed at 100 °C for 10 min, and then heated to 300 °C and maintained for 1 h under Argon protection. After the solution was cooled naturally, nanocrystals were precipitated from the solution with ethanol, and washed with ethanol/water (1:1 v/v) thrice. 0.1 mL CO-520, 6 mL cyclohexane and 4 mL 0.01 M $NaYF_4$:Yb,Tm core nanocrystal solution in cyclohexane were mixed and stirred for 10 min. Then 0.4 mL CO-520 and 0.08 mL ammonia (wt 30%) were added and the container was sealed and sonicated for 20 min until a transparent emulsion was formed. 0.04 mL TEOS was then added into the solution, and the solution was rotated for two days at a speed of 600 rpm. $NaYF_4$:Yb,Tm@SiO_2 nanoparticles were precipitated by adding acetone, washed with ethanol/water (1:1 v/v) twice and then stored in water. For further coating of an amorphous TiO_2 layer, amino groups were initially modified on the silica surface by grafting (3-aminopropyl)-trimethoxysilane (APS) on the $NaYF_4$:Yb,Tm@SiO_2 nanoparticles. In a typical synthesis of TiO_2-UCN nanoparticles, 0.02 mmol $NaYF_4$:Yb,Tm@SiO_2 nanoparticles was dispersed in 10 mL isopropanol, 0.3 mL ammonia (28 wt%) and 2.5 mL water. Then, 2 mL of

Journal of Materials Chemistry B Accepted Manuscript

titanium diisopropoxide bis(acetylacetonate) solution (0.001 M in isopropanol) was slowly added into the above solution and stirred for 24 h at RT (20 ºC). Amorphous TiO_2 coated nanoparticles were then collected by centrifugation and washed with isopropanol twice. To achieve a crystallized TiO_2 shell, the TiO_2-UCN nanoparticles were treated in ethanol in a sealed autoclave at 180 ºC for 24 h under an air atmosphere.

Characterization of TiO_2-UCN: Transmission electron microscopy (TEM) and EDX spectroscopy were performed on a JEOL 2010F TEM (Jeol Ltd., Tokyo, Japan). Powder X-ray diffraction (XRD) was carried out on a Philips X' Pert Pro X-ray diffractometer equipped with a Cu Kα radiation. For fluorescent study of the particles in different physiological solutions, 1 mg of TiO_2-UCN were resuspended in 1.5 mL of the respective solution of either water, PBS or DMEM culture medium with or without 10 % fetal bovine serum supplementation. For fluorescent study of the particles soaked in water and acidic water over time, 1 mg of TiO_2-UCN were resuspended in 1 mL of either water or acidified water at pH 4 for 0, 1, 2 and 3.5 h. Fluorescence spectra of the nanoparticle suspension under 980 nm laser excitation was then measured with a SpectroPro 2150i spectrophotometer (Roper Scientific Acton Research, MA) equipped with a 1200 g mm^{-1} grating and a continuous wave (CW) 980 nm diode laser.

Detection of ROS production from TiO_2-UCN: In a typical experiment, 1 mg of the TiO_2-UCN was suspended in 2 mL of water containing 10 μM of APF dye. In the scavenger experiment to verify the type of ROS produced from photoinduced TiO_2-UCN, pre-optimized amount of either 10 mM sodium pyruvate, 1.4 M DMSO, 100 mM Tiron or 100 mM sodium azide – the respective scavengers for hydrogen peroxide, hydroxyl radical, superoxide anion and singlet oxygen - was additionally included in the mixture. The mixture was then placed in a cuvette and the solution was irradiated with a 980 nm laser (EINST Technology Pte Ltd,

Journal of Materials Chemistry B Accepted Manuscript

Singapore) at 2.16 W cm^{-2} for 20 min time intervals beginning from time (t) = 0 to 60 min, with the fluorescence emission of APF at 520 nm (upon excitation at 485 nm) being measured between intervals using a FLUOstar OPTIMA fluorescence plate reader (BMG LABTECH GmbH, Germany). For the verification study on singlet oxygen production from NIR-irradiated TiO_2-UCN, 0.5 mg or 2.5 mg of nanoparticle was suspended in 2 mL of water containing 10 μM of singlet oxygen sensor green dye (instead of APF dye) and then irradiated with a 980 nm laser and the dye fluorescence read in the same manner as previously described.

Dynamic light scattering for measurement of particle hydrodynamic size: The size distribution of the nanoparticles were measured with a Malvern zetasizer nano series (Malvern Instruments Ltd., Worcestershire, UK).

Cell culture: Human oral squamous cell carcinoma (CAL-27) (OSCC) and normal human lung fibroblasts (IMR-90) (NHF) cells were obtained from American Type Culture Collection (ATCC, Manassas, VA, USA) and grown in RPMI and DMEM culture medium respectively, supplemented with 10 % fetal bovine serum, 100 units mL^{-1} of penicillin and 100 μg mL^{-1} of streptomycin, and maintained in a humidified, 5 % carbon dioxide (CO_2) atmosphere at 37 °C.

Cell imaging study: Cells were plated onto a 8 well chambered slide at a density of 8,000 cells $well^{-1}$ for overnight at 37 °C in a humidified, 5 % CO_2 atmosphere. They were then treated with 54 μg mL^{-1} of TiO_2-UCN for 6 h at 37 °C. After which, the old culture medium containing unbound and non-internalized nanoparticles were discarded and the cells were washed thrice with PBS before they were fixed in ice-cold methanol for 10 min. The cell membrane and nuclei were counterstained with Wheat Germ Agglutinin, Alexa Fluor® 488 Conjugate and propidium iodide, respectively. Stained cells were imaged under a 40x objective of a Nikon 80i Fluorescence Microscope (Nikon, Tokyo, Japan) equipped with a

Journal of Materials Chemistry B Accepted Manuscript

980 nm Laser Wide-field Fluorescence add-on (EINST Technology Pte Ltd, Singapore). The power density of the 980 nm laser falling on the cell sample under the 40x objective is ~ 326 W cm^{-2}.

Dark-toxicity test: Cells were plated onto a 96-well plate at a density of 8,000 cells $well^{-1}$ for overnight at 37 °C in a humidified, 5 % CO_2 atmosphere. A 1 mg mL^{-1} TiO_2-UCN stock solution was prepared in PBS and dispersed by sonication for 20 min before being diluted out in the respective culture medium to a concentration ranging from 0 to 270 μg mL^{-1}. The cells were treated with the different concentration of nanoparticles for 6 h at 37 °C followed by thrice washing in PBS to remove unbound and non-internalized nanoparticles. Fresh culture medium was then added into each well and the cells were returned to 5 % CO_2 atmosphere at 37 °C for another 24 h round of incubation. The number of cells that remained viable was then assessed by CellTiter 96® AQ_{ueous} One Solution Cell Proliferation Assay (Promega, Madison, WI, USA) as per manufacturer's instructions. Cell viability is expressed as a percentage of control cells without exposure to TiO_2-UCN.

In vitro PDT: Cells were plated and treated with TiO_2-UCN as described in the dark-toxicity test above. After washing off the nanoparticles thrice in PBS and replacing it with fresh culture medium, the cells were exposed to a 980 nm laser (2.1 W cm^{-2}) for 5 min 20 s. They were then returned to 5 % CO_2 atmosphere at 37 °C for another 24 h before assessing the number of viable cells using the CellTiter 96® AQ_{ueous} One Solution Cell Proliferation Assay (Promega, Madison, WI, USA). Cell viability is expressed as a percentage of control cells without exposure to TiO_2-UCN and laser.

4. Conclusion

Journal of Materials Chemistry B Accepted Manuscript

We presented a core-shell nanocomposite of UCN core uniformly coated with a continuous layer of TiO_2 shell. The UCN core acts as a light transducer to convert safe and deeply penetrating NIR light to higher-energy visible and UV wavelengths that matches the activation absorption spectrum of the coated TiO_2 photocatalyst. Photoinduced TiO_2 by the upconverted UV light results in the generation of more than one type of ROS that includes hydroxyl radicals, superoxide anions and hydrogen peroxide. The TiO_2-UCN composite produced a stable amount of these ROS when stored at 4 °C as dry powder or soaked in EtOH for at least over a month. Their potential as an agent of PDT in inducing cell death was also successfully demonstrated *in vitro*. By having the potential to overcome the limitation of penetration depth in conventional PDT, TiO_2-UCN can be used for the treatment of thick, bulky or deep-seated tumors, thereby offering PDT as a treatment option for a larger range of tumor sizes, types and locations.

Acknowledgements

We thank S.H.Q. Chan (Department of Biomedical Engineering, Faculty of Engineering, National University of Singapore) for working on the stability and type of ROS produced. We acknowledge financial support from Singapore Agency for Science, Technology and Research (A*STAR) Biomedical Engineering Programme (grant R-397-000-128-305) and National University of Singapore. S.S. Lucky is a recipient of NGS scholarship from NUS graduate school (NGS) for Integrative Sciences and Engineering, National University of Singapore.

References

1. Y. W. Naguib and Z. Cui, *Adv. Exp. Med. Biol.*, 2014, **811**, 207-233.
2. A. K. Parchur, A. A. Ansari, B. P. Singh, T. N. Hasan, N. A. Syed, S. B. Rai and R. S. Ningthoujam, *Integrative Biology*, 2014, **6**, 53-64.
3. A. Master, M. Livingston and A. Sen Gupta, *J. Controlled Release*, 2013, **168**, 88-102.
4. A. Fujishima and K. Honda, *Nature*, 1972, **238**, 37-38.

Journal of Materials Chemistry B Accepted Manuscript

5. T. Matsunaga, R. Tomoda, T. Nakajima and H. Wake, *FEMS Microbiol. Lett.*, 1985, **29**, 211-214.
6. T. Matsunaga, R. Tomoda, T. Nakajima, N. Nakamura and T. Komine, *Appl. Environ. Microbiol.*, 1988, **54**, 1330-1333.
7. M. Fujihira, Y. Satoh and T. Osa, *Nature*, 1981, **293**, 206-208.
8. T. Inoue, A. Fujishima, S. Konishi and K. Honda, *Nature*, 1979, **277**, 637-638.
9. J. S. Chen, M. C. Liu, L. Zhang, J. D. Zhang and L. T. Jin, *Water Res.*, 2003, **37**, 3815-3820.
10. A. P. Zhang and Y. P. Sun, *World J Gastroenterol.*, 2004, **10**, 3191-3193.
11. Y. Kubota, T. Shuin, C. Kawasaki, M. Hosaka, H. Kitamura, R. Cai, H. Sakai, K. Hashimoto and A. Fujishima, *Br. J. Cancer*, 1994, **70**, 1107-1111.
12. R. X. Cai, Y. Kubota, T. Shuin, H. Sakai, K. Hashimoto and A. Fujishima, *Cancer Res.*, 1992, **52**, 2346-2348.
13. J. Xu, Y. Sun, Y. M. Zhao, J. J. Huang, C. M. Chen and Z. Y. Jiang, *International Journal of Photoenergy*, 2007.
14. C. Wang, S. Q. Cao, X. X. Tie, B. Qiu, A. H. Wu and Z. H. Zheng, *Mol. Biol. Rep.*, 2011, **38**, 523-530.
15. Y. S. Lee, S. Yoon, H. J. Yoon, K. Lee, H. K. Yoon, J. H. Lee and C. W. Song, *Toxicol. Lett.*, 2009, **189**, 191-199.
16. T. Y. Lai and W. C. Lee, *Journal of Photochemistry and Photobiology a-Chemistry*, 2009, **204**, 148-153.
17. D. R. Sandeman, *Br. J. Radiol.*, 1988, **61**, 740-740.
18. S. L. Jacques, D. R. Weaver and S. M. Reppert, *Photochem. Photobiol.*, 1987, **45**, 637-641.
19. J. V. Frangioni, *Current opinion in chemical biology*, 2003, **7**, 626-634.
20. F. Auzel, *Chem. Rev.*, 2004, **104**, 139-173.
21. R. Abdul Jalil and Y. Zhang, *Biomaterials*, 2008, **29**, 4122-4128.
22. D. Bechet, P. Couleaud, C. Frochot, M. L. Viriot, F. Guillemin and M. Barberi-Heyob, *Trends in biotechnology*, 2008, **26**, 612-621.
23. D. K. Chatterjee, M. K. Gnanasammandhan and Y. Zhang, *Small*, 2010, **6**, 2781-2795.
24. L. Cheng, C. Wang and Z. Liu, *Nanoscale*, 2013, **5**, 23-37.
25. B. Dong, S. Xu, J. Sun, S. Bi, D. Li, X. Bai, Y. Wang, L. Wang and H. Song, *Journal of Materials Chemistry*, 2011, **21**, 6193-6200.
26. M. K. Jayakumar, N. M. Idris and Y. Zhang, *Proceedings of the National Academy of Sciences of the United States of America*, 2012, **109**, 8483-8488.
27. F. Wang and X. G. Liu, *J. Am. Chem. Soc.*, 2008, **130**, 5642-5643.
28. W. Li, J. Wang, J. Ren and X. Qu, *J. Am. Chem. Soc.*, 2014, **136**, 2248-2251.
29. Z. Liu, E. Ju, J. Liu, Y. Du, Z. Li, Q. Yuan, J. Ren and X. Qu, *Biomaterials*, 2013, **34**, 7444-7452.
30. N. M. Idris, M. K. Jayakumar, A. Bansal and Y. Zhang, *Chem Soc Rev*, 2014.
31. W. L. Wang, Q. K. Shang, W. Zheng, H. Yu, X. J. Feng, Z. D. Wang, Y. B. Zhang and G. Q. Li, *Journal of Physical Chemistry C*, 2010, **114**, 13663-13669.
32. Q. C. Xu, Y. Zhang, M. J. Tan, Y. Liu, S. J. Yuan, C. Choong, N. S. Tan and T. T. Y. Tan, *Advanced Healthcare Materials*, 2012, **1**, 470-474.
33. Y. N. Tang, W. H. Di, X. S. Zhai, R. Y. Yang and W. P. Qin, *ACS Catalysis*, 2013, **3**, 405-412.
34. Z. Q. Li, C. L. Li, Y. Y. Mei, L. M. Wang, G. H. Du and Y. J. Xiong, *Nanoscale*, 2013, **5**, 3030-3036.
35. Z. Q. Li, Y. Zhang and S. Jiang, *Adv. Mater.*, 2008, **20**, 4765-4769.
36. M. Saif and M. S. A. Abdel-Mottaleb, *Inorg. Chim. Acta*, 2007, **360**, 2863-2874.

Journal of Materials Chemistry B Accepted Manuscript

37. Y. Murakami, E. Kenji, A. Y. Nosaka and Y. Nosaka, *J. Phys. Chem. B*, 2006, **110**, 16808-16811.
38. Y. Nosaka, M. Nakamura and T. Hirakawa, *PCCP*, 2002, **4**, 1088-1092.
39. W. Kubo and T. Tatsuma, *Anal. Sci.*, 2004, **20**, 591-593.
40. M. Buchalska, P. Labuz, L. Bujak, G. Szewczyk, T. Sarna, S. Mackowski and W. Macyk, *Dalton Transactions*, 2013, **42**, 9468-9475.
41. T. Daimon and Y. Nosaka, *Journal of Physical Chemistry C*, 2007, **111**, 4420-4424.
42. T. Hirakawa, T. Daimon, M. Kitazawa, N. Ohguri, C. Koga, N. Negishi, S. Matsuzawa and Y. Nosaka, *Journal of Photochemistry and Photobiology a-Chemistry*, 2007, **190**, 58-68.
43. T. Hirakawa, H. Kominami, B. Ohtani and Y. Nosaka, *J. Phys. Chem. B*, 2001, **105**, 6993-6999.
44. Y. Nosaka, T. Daimon, A. Y. Nosaka and Y. Murakami, *PCCP*, 2004, **6**, 2917-2918.
45. T. Daimon, T. Hirakawa, M. Kitazawa, J. Suetake and Y. Nosaka, *Applied Catalysis a-General*, 2008, **340**, 169-175.
46. A. Juzeniene and J. Moan, *Photodiagnosis and Photodynamic Therapy*, 2007, **4**, 3-11.
47. M. Ochsner, *Journal of Photochemistry and Photobiology B-Biology*, 1996, **32**, 3-9.
48. D. S. Mao, G. Z. Lu and Q. L. Chen, *Chinese Journal of Catalysis*, 2005, **26**, 271-276.
49. Z. Q. Li and Y. Zhang, *Nanotechnology*, 2008, **19**, 345606-345610.

Journal of Materials Chemistry B Accepted Manuscript

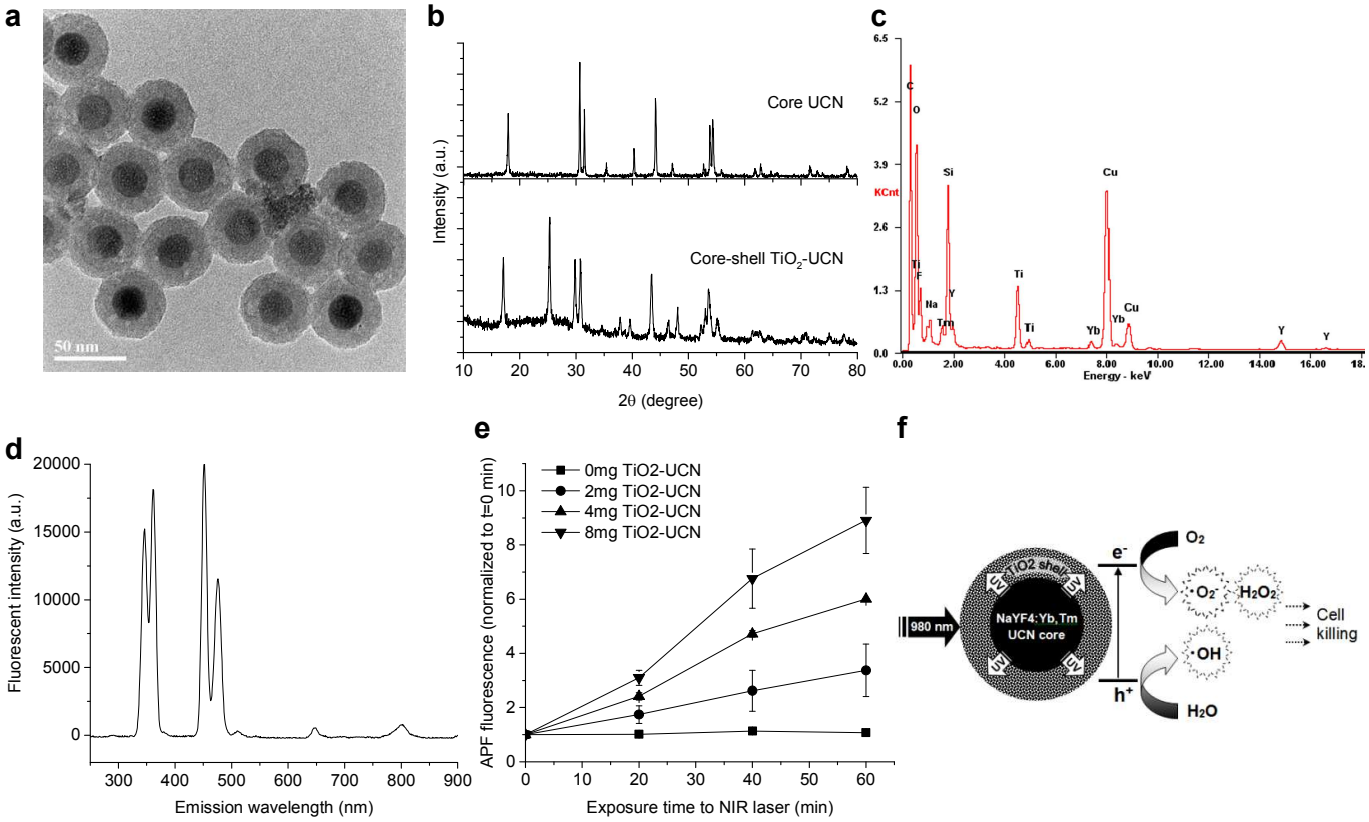

Figure 1. TiO_2-coated $NaYF_4$:Yb,Tm UCN as an agent of PDT. (**a**) TEM image of TiO_2-UCN (scale bar, 50 nm). (**b**) XRD patterns of core UCN and core-shell TiO_2-UCN. (**c**) EDX spectrum of the TiO_2-coated $NaYF_4$:Yb,Tm particles supported on a carbon-film coated copper grid. The peaks labeled Na, Y, F, Yb and Tm originate from the core nanocrystals, while that of Ti, Si and O come from the shells. The elements C and Cu are from the carbon-film coated copper grid used in the TEM and EDX characterizations. (**d**) Fluorescence emission spectrum of 1 mg of TiO_2-UCN suspended in 1.5 mL water, under 980 nm excitation. (**e**) ROS production from 0, 2, 4 and 8 mg of TiO_2-UCN suspended in 2 mL of water, under 980 nm irradiation (2.16 W cm^{-2}). Values are means (n=2) ± s.e.m. (**f**) Schematic illustration on the mechanism of TiO_2-UCN to generate ROS for PDT (not to scale). After

Journal of Materials Chemistry B Accepted Manuscript

excitation by a NIR light at 980 nm, the UCN upconvert the NIR light to UV and visible light of different wavelengths, as seen in d. Spectral overlap between the emitted UV and maximum absorption wavelength of the coated TiO_2 activates the TiO_2 shell to generate an e^--h^+ pair as its electron gets excited from the valence band to the conduction band. The resultant hole oxidizes a water (H_2O) molecule to yield hydroxyl radical (·OH), while the electron reduces oxygen (O_2) to give superoxide anion ($\cdot O_2^-$) or hydrogen peroxide (H_2O_2). This elevated amount of cytotoxic ROS can be used to kill cells for PDT.

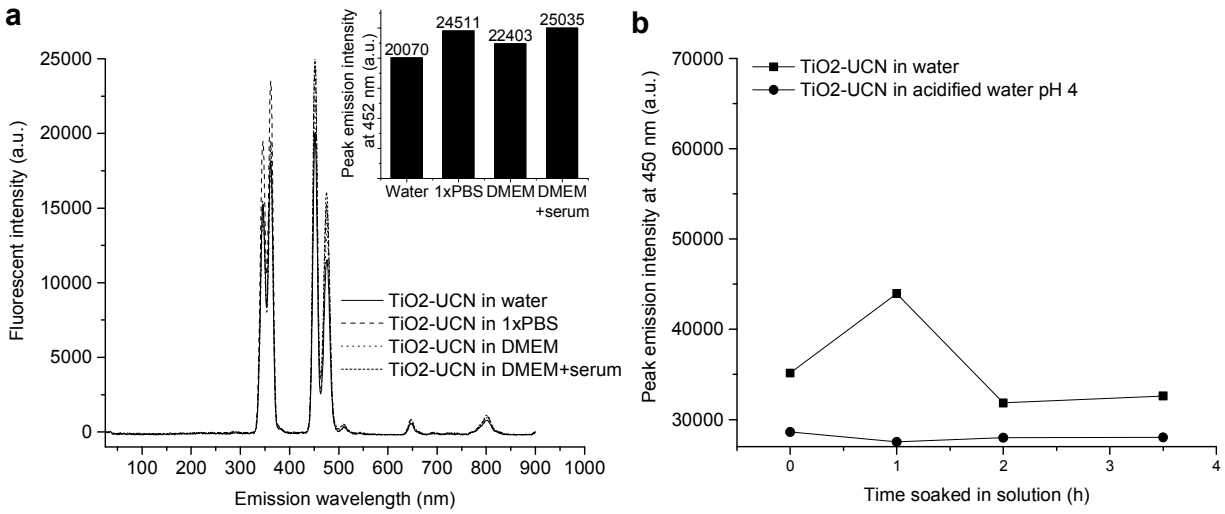

Figure 2. Stability of TiO_2-UCN fluorescence. (**a**) Fluorescence emission spectrum of 1 mg of TiO_2-UCN suspended in 1.5 mL of different physiological solutions under 980 nm laser excitation. Inset shows peak emission intensity at 452 nm to highlight the insignificant change in intensity in the different solutions. (**b**) Peak emission intensity at 450 nm (under 980 nm laser excitation) of 1 mg of TiO_2-UCN soaked in 1 mL of water or acidic water over several hours.

Journal of Materials Chemistry B Accepted Manuscript

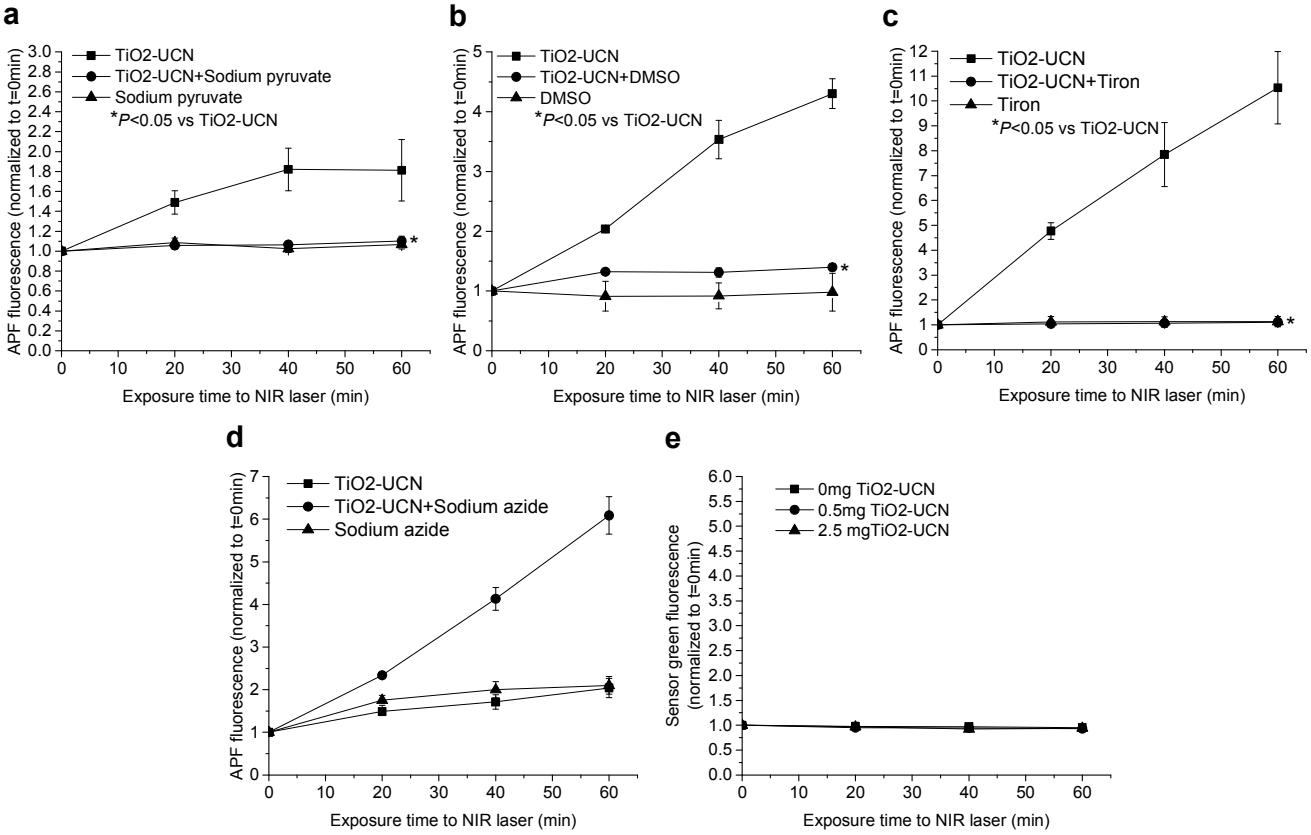

Figure 3. Type of ROS produced from NIR-irradiated TiO_2-UCN suspension in water (1 mg TiO_2-UCN in 2 mL water). Presence of (**a**) hydrogen peroxide, (**b**) hydroxyl radical, (**c**) superoxide anion and (**d**) singlet oxygen species produced was detected by fluorescence quenching of the APF dye upon addition of their respective scavengers - sodium pyruvate, DMSO, Tiron and sodium azide - into the suspension of TiO_2-UCN irradiated with the 980 nm NIR laser (2.16 W cm^{-2}). APF fluorescence is plotted as a function of exposure time (t) to the 980 nm NIR laser. Values are means (n=2) ± s.e.m. **P* < 0.05 compared to NIR-irradiated TiO_2-UCN without scavenger addition. (**e**) Verification study on singlet oxygen production from NIR-irradiated TiO_2-UCN by fluorescence of a fluorogenic marker specific for singlet oxygen – singlet oxygen sensor green dye. Two concentrations of the nanoparticles were used – 0.5 mg or 2.5 mg TiO_2-UCN in 2 mL of water. The dye fluorescence is plotted as a function of exposure time (t) to the 980 nm NIR laser.

Journal of Materials Chemistry B Accepted Manuscript

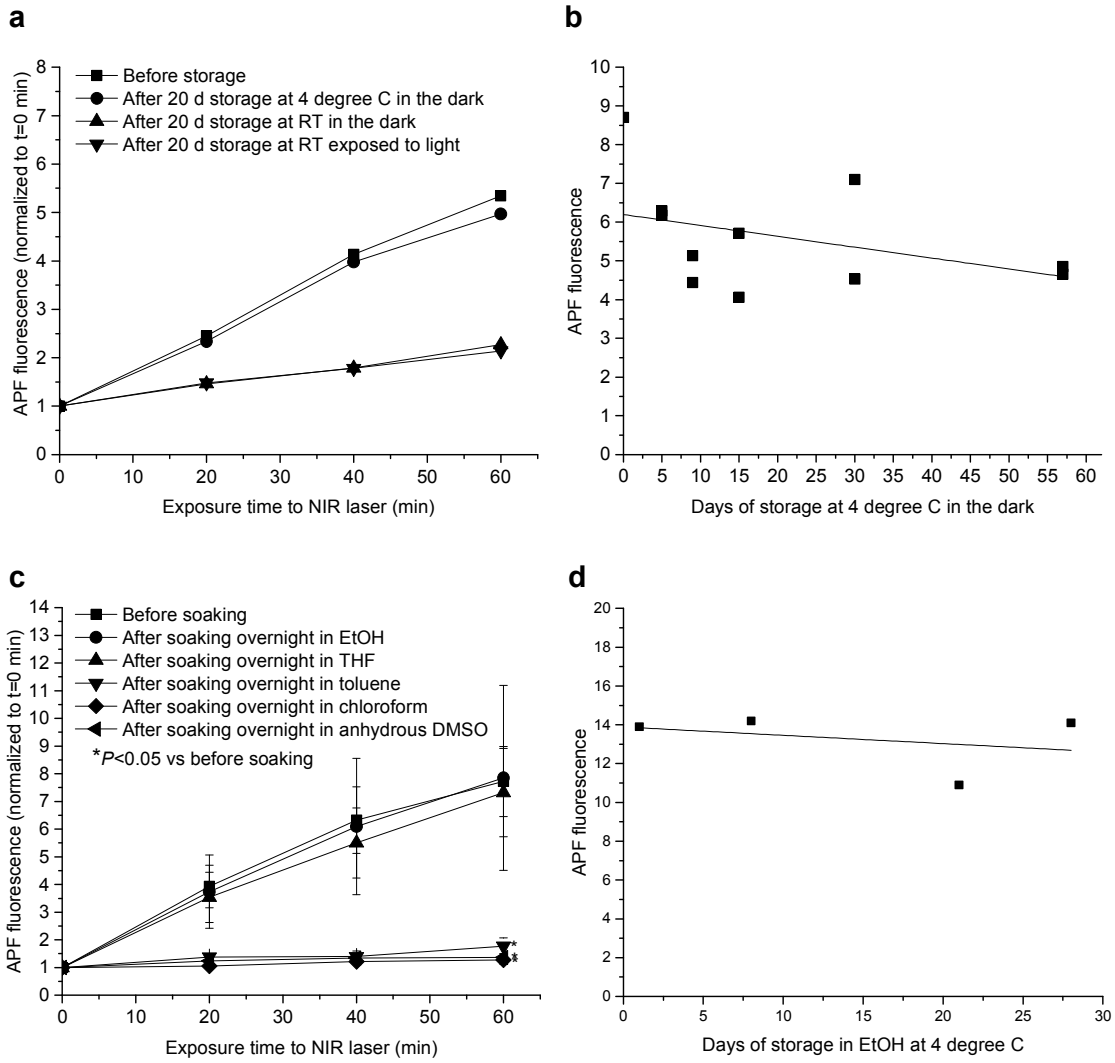

Figure 4. ROS production from TiO_2-UCN stored at different conditions. (**a**) TiO_2-UCN activity for ROS production under 980 nm irradiation (2.16 W cm^{-2}) after 20 days of storage as dry powder at either 4 °C in the dark, RT in the dark or RT but exposed to light. (**b**) Shelf life of TiO_2-UCN stored as dry powder at 4 °C in the dark as determined by its ROS production under 60 min of 980 nm irradiation (2.16 W cm^{-2}). Linear fit line shows trend in ROS production over 57 days. (**c**) ROS production from 980 nm-irradiated (2.16 W cm^{-2}) TiO_2-UCN after soaked overnight in either EtOH, THF, toluene, chloroform or anhydrous DMSO. The respective solvents were removed and the TiO_2-UCN resuspended in water prior

Journal of Materials Chemistry B Accepted Manuscript

to the ROS test. Values are means (n=3) ± s.e.m. *$P < 0.05$ compared to before soaking. (**d**) Long-term effect of storing TiO_2-UCN in EtOH at 4 °C as determined by its ROS production under 60 min of 980 nm irradiation (2.16 W cm^{-2}). Linear fit line shows trend in ROS production over 4 weeks. The storage medium, EtOH, was removed and the TiO_2-UCN resuspended in water prior to the ROS test. ROS production was determined by APF fluorescence from a suspension of 1 mg of TiO_2-UCN in 2 mL water containing 10 μM of APF dye in all experiments.

Journal of Materials Chemistry B Accepted Manuscript

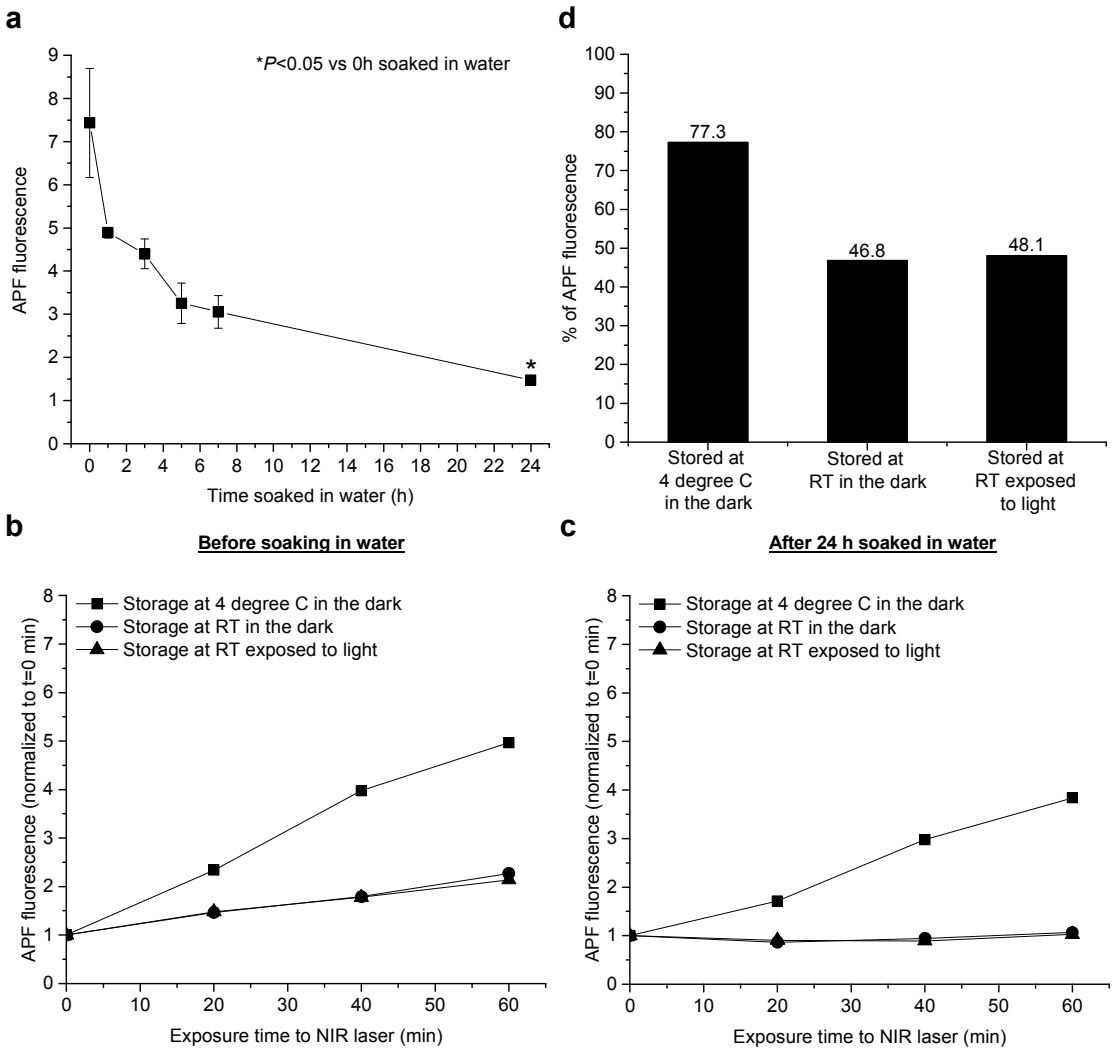

Figure 5. Stability of TiO_2-UCN activity for ROS production when soaked in water. (**a**) ROS production from 980 nm NIR-irradiated TiO_2-UCN (at 2.16 W cm^{-2} for 60 min) soaked in water for up to 24 h was monitored by APF fluorescence and plotted as a function of time soaked in the water. Values are means (n=2) ± s.e.m. **P* < 0.05 compared to 0 h soaked in water. ROS production from 980 nm NIR-irradiated TiO_2-UCN (at 2.16 W cm^{-2} for 60 min) (**b**) before soaking and (**c**) after 24 h soaked in water at either 4 °C in the dark, RT in the dark or RT but exposed to light was determined by APF fluorescence and plotted as a function of exposure time (t) to the 980 nm NIR laser. (**d**) Drop in TiO_2-UCN activity for ROS

Journal of Materials Chemistry B Accepted Manuscript

production is chartered as the percentage of APF fluorescence after 24 h soaked in water (shown in **c**) divided by the APF fluorescence before soaking in water (shown in **b**) for each of the different storage condition. ROS production was determined by APF fluorescence from a suspension of 1 mg of TiO_2-UCN in 2 mL water containing 10 μM of APF dye in all experiments.

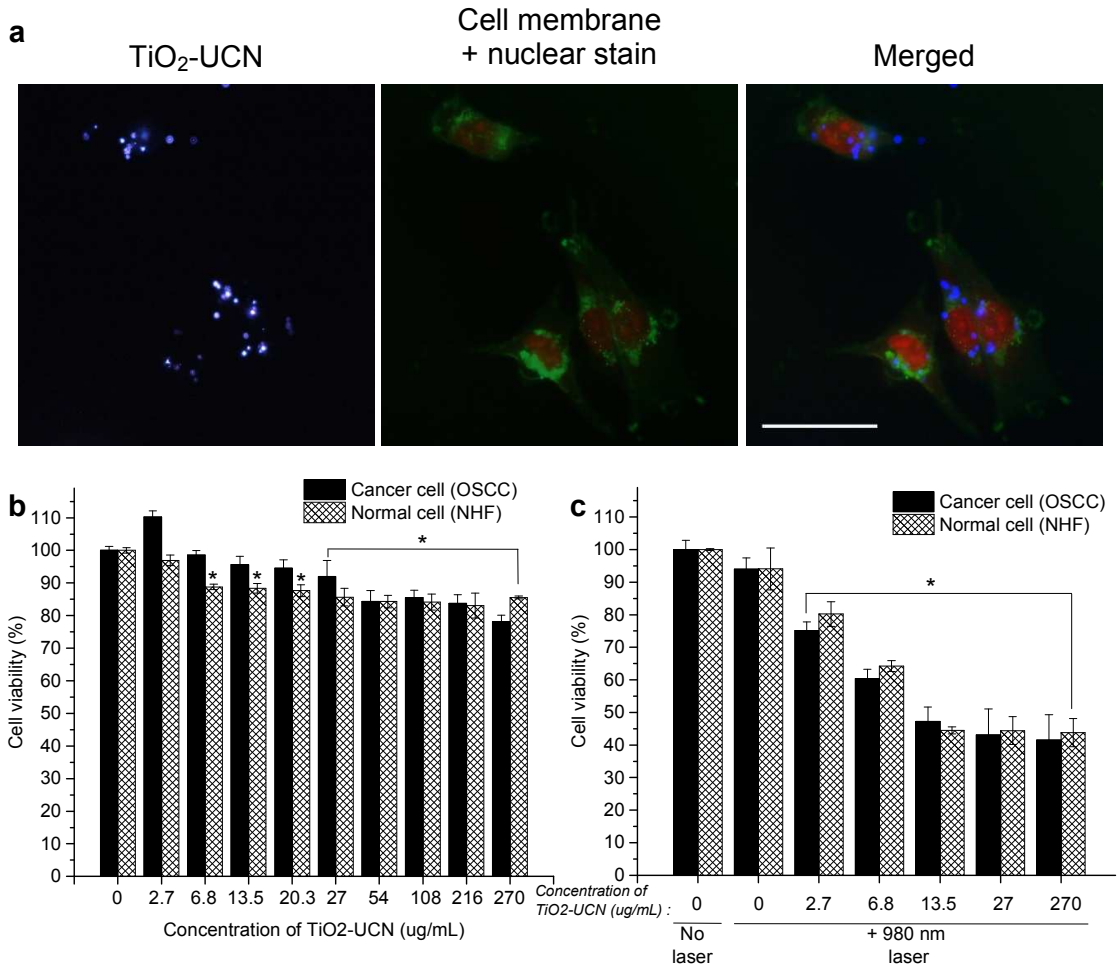

Figure 6. TiO_2-UCN as an agent of PDT *in vitro*. (**a**) Uptake of TiO_2-UCN into OSCC as captured by fluorescence cell imaging. Blue fluorescence indicates upconversion emission from the TiO_2-UCN under 980 nm excitation, green fluorescence indicates cell membrane counterstaining with Wheat Germ Agglutinin, Alexa Fluor® 488 Conjugate while red fluorescence is nuclear counterstaining with propidium iodide (scale bar: 50 μm). (**b**) Dark-

Journal of Materials Chemistry B Accepted Manuscript

toxicity of TiO_2-UCN incubated with cancer cells, OSCC and normal cells, NHF for 6 h. Values are means (n=3) ± s.d. *$P < 0.05$ compared to control cells without exposure to TiO_2-UCN. (**c**) *In vitro* PDT using TiO_2-UCN on OSCC and NHF cells. Values are means (n=3) ± s.d. *$P < 0.05$ compared to control cells treated with the respective concentration of TiO_2-UCN but without exposure to 980 nm laser (i.e. dark-toxicity values).

Journal of Materials Chemistry B Accepted Manuscript

Table of contents entry

Titania-coated upconversion nanoparticle converts 980nm to UV light for activation of coated titania to generate reactive oxygen species against cells.

Keywords: Titanium dioxide, upconversion, near-infrared, reactive oxygen species, photodynamic therapy.

N.M. Idris, S.S. Lucky, Z. Li, K. Huang, Y. Zhang*

Photoactivation of Core-Shell Titania Coated Upconversion Nanoparticles and its Effect on Cell Death

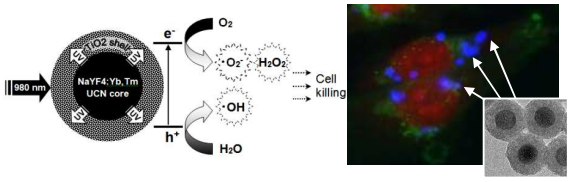

Journal of Materials Chemistry B Accepted Manuscript